



Cite this: DOI: 10.1039/d5ea00083a

## A significant source of nitrous oxide from recreational use in Ho Chi Minh City, a future Southeast Asian megacity in Vietnam

Grant Forster,<sup>ID \*ab</sup> Michael Biggart,<sup>cd</sup> Ruth M. Doherty,<sup>c</sup> Alex R. Baker,<sup>b</sup> Alex Etchells,<sup>e</sup> Graham Mills,<sup>b</sup> To Thi Hien,<sup>\*fg</sup> Nguyen Doan Thien Chi,<sup>fg</sup> Duong Huu Huy<sup>h</sup> and David Oram<sup>ab</sup>

The first *in situ* observations of nitrous oxide ( $\text{N}_2\text{O}$ ) mole fraction for Ho Chi Minh City are presented for October 2018 to March 2019. The time series of  $\text{N}_2\text{O}$  observations made from the roof of a 10-storey building was dominated by elevated  $\text{N}_2\text{O}$  mole fractions with a maximum of  $613 \text{ nmol mol}^{-1}$  in air arriving from the northeast and east. The diurnal pattern of  $\text{N}_2\text{O}$  did not follow the general pattern of other pollutants (i.e., carbon monoxide) associated with urban anthropogenic activity, such as emissions from traffic. The observations revealed an underlying mean daily diurnal cycle with an amplitude of approximately  $10 \text{ nmol mol}^{-1}$ , consistent with the accumulation of  $\text{N}_2\text{O}$  overnight in a shallow boundary layer. An exception to this was the extremely elevated mean diurnal cycle observed for the northeast sector, where a magnitude of  $\sim 45 \text{ nmol mol}^{-1}$  indicates a strong local source. Using 'discrete' sampling, an area of elevated  $\text{N}_2\text{O}$  (mean  $4733 \text{ nmol mol}^{-1}$ ) was identified in an area of the city, the Bùi Viện Walking Street, where  $\text{N}_2\text{O}$  is used for recreational purposes, a practice that is raising serious health concerns globally. Using a simple 'bottom-up' approach, estimates of the emission of  $\text{N}_2\text{O}$  from this activity were  $0.021 \pm 0.010 \text{ Gg per year}$ , an emission comparable to the estimated  $\text{N}_2\text{O}$  emissions from the stationary energy sector in HCMC. To investigate this further, the ADMS-Urban dispersion model was used to simulate the *in situ* observations of  $\text{N}_2\text{O}$  for the measurement site. It was found that the diurnal cycle for each wind sector was reproducible when the emissions of  $\text{N}_2\text{O}$  were assumed to be coming from the Bùi Viện Walking Street; however, the model emissions required for this were approximately one order of magnitude higher than those estimated using the 'bottom-up' approach. Despite the disagreement in the magnitude of emissions, continued measurements at the same site could be used to assess the effectiveness of the nationwide ban on  $\text{N}_2\text{O}$  for recreational purposes, as they represent a baseline before the nationwide ban introduced in 2025. Additionally, it is suggested that care must be taken when using atmospheric observations of  $\text{N}_2\text{O}$  and CO to derive excess  $\text{N}_2\text{O}/\text{CO}$  molar emission ratios from traffic in tropical Southeast Asian cities. For example, despite being attributed as the largest source of  $\text{N}_2\text{O}$  in HCMC, the observations presented herein show no observable  $\text{N}_2\text{O}$  increase from local rush hour traffic peaks characterised by high CO, likely due to the precision limits of the analyser. Finally, the work presented herein emphasises some of the challenges encountered when estimating emissions of greenhouse gases from heterogeneous sources in urban environments.

Received 22nd July 2025  
 Accepted 22nd December 2025

DOI: 10.1039/d5ea00083a  
[rsc.li/esatmospheres](http://rsc.li/esatmospheres)

<sup>a</sup>National Centre for Atmospheric Sciences (NCAS), School of Environmental Sciences, University of East Anglia, Norwich, NR4 7TJ, UK. E-mail: grant.forster@ncas.ac.uk

<sup>b</sup>Centre for Ocean and Atmospheric Science, School of Environmental Sciences, University of East Anglia, Norwich, NR4 7TJ, UK

<sup>c</sup>School of Geosciences, University of Edinburgh, Edinburgh, EH9 3JW, UK

<sup>d</sup>Centre for Atmospheric Science, University of Manchester, Manchester, M13 9P, UK

<sup>e</sup>Research and Specialist Computing Support, IT & Computing Services, University of East Anglia, Norwich, NR4 7TJ, UK

<sup>f</sup>Faculty of Environment, University of Science, 227 Nguyen Van Cu Street, District 5, Ho Chi Minh City, Vietnam. E-mail: tohien@hcmus.edu.vn

<sup>g</sup>Vietnam National University, Ho Chi Minh City, Vietnam

<sup>h</sup>Faculty of Food Science and Technology, Ho Chi Minh City University of Food Industry, 140 Le Trong Tan Street, Tan Phu District, Ho Chi Minh City, Vietnam

### Environmental significance

This article has environmental significance as we report the first *in situ* urban atmospheric measurements of nitrous oxide from Vietnam and identify a large urban source of nitrous oxide originating from recreational drug use in Ho Chi Minh City. Nitrous oxide is the third most important greenhouse gas and very little work has been done looking at urban emissions. This source of nitrous oxide should be considered when mitigating urban emissions as recreational use of nitrous oxide is on the rise in many parts of the world.



## 1. Introduction

The Paris Agreement within the United Nations Framework Convention on Climate Change<sup>1</sup> was signed in 2016 by 196 countries. This legally binding international treaty requires governments to pursue efforts to limit the global temperature increase to 1.5 °C through the reduction in the emissions of greenhouse gases (GHG). One greenhouse gas that will be targeted through mitigation strategies across global and regional scales is nitrous oxide (N<sub>2</sub>O). Nitrous oxide is a long-lived greenhouse gas with an atmospheric lifetime of approximately 110 years.<sup>2</sup> Over a 100-year time horizon, N<sub>2</sub>O is 273 times more effective at trapping infrared radiation than carbon dioxide, as reflected in its high Global Warming Potential.<sup>3</sup> Since the industrial revolution, the mole fraction global mean of atmospheric N<sub>2</sub>O has increased from 270 nmol mol<sup>-1</sup> in 1750 to 337.71 nmol mol<sup>-1</sup> in 2024 (ref. 4) and is currently the third biggest contributor to enhanced radiative forcing behind carbon dioxide and methane (CH<sub>4</sub>). In addition to the effects on radiative forcing, anthropogenic emission of N<sub>2</sub>O is important in the destruction of stratospheric ozone (O<sub>3</sub>).<sup>5</sup> Despite the importance of N<sub>2</sub>O, its global budget remains poorly constrained due to the complexity of natural and anthropogenic sources. Natural sources of atmospheric N<sub>2</sub>O are primarily from microbial production (nitrification and denitrification) in the soils and oceans, with the anthropogenic sources dominated by emissions from agricultural activity.<sup>6-8</sup> The natural microbial action in soils has been perturbed by nitrogen fertiliser, causing an estimated 30% increase in N<sub>2</sub>O emission over the past four decades; estimated total global emissions of 17.0 (range: 12.2–23.5) teragrams (10<sup>12</sup> grams) of nitrogen (in N<sub>2</sub>O) per year (TgN per year) and 16.9 (range: 15.9–17.7) TgN per year using 'bottom-up' and 'top-down' methods, respectively.<sup>9</sup> The uncertainty range in these estimates reflects the uncertainties associated with quantifying global emissions using different sophisticated accounting techniques (e.g. inventory, statistical extrapolation of flux measurements, process-based land and ocean modelling).

It has been estimated that cities and urbanized areas are responsible for more than two-thirds of greenhouse gas emissions globally<sup>10–12</sup> with a recent study suggesting that just 25 megacities, defined as cities with more than 10 million people, are responsible for approximately 52% of the world's urban greenhouse gas emissions.<sup>13</sup> This suggests that the successful implementation of greenhouse gas mitigation strategies worldwide will require a better understanding of the sources and magnitudes of urban greenhouse gas emissions.

Vietnam represents one of the fastest-growing economies in Southeast Asia and, as a result, has undergone rapid urbanisation, industrialisation, and population growth. In turn, this has led to increased emissions of greenhouse gases, primarily because of a rapid increase in energy demand.<sup>14</sup> The latest submission from Vietnam to the UNFCCC reported CO<sub>2</sub> equivalent emissions of approximately 284 Mt (10<sup>6</sup> tonnes) for 2014, an increase of 250% from values reported in 1990, with a projected rise to 927.9 Mt by 2030 under a business-as-usual

scenario.<sup>15</sup> However, through their Nationally Determined Contributions, Vietnam has committed to reducing greenhouse gas emissions by 15.8% with domestic resources and by 43.5% with international support by 2030 and achieving net-zero carbon emissions by 2050.<sup>15</sup>

With more than 9 million people (13 million in the metropolitan area), Ho Chi Minh City (HCMC) is a rapidly developing Vietnamese sub-tropical city predicted to become a megacity in the next decade. To address the issue of urban greenhouse gas emissions and to strengthen its commitment to the Paris 2015 Agreement, HCMC is a member of the Global Covenant of Mayors for Climate and Energy and is committed to achieving ambitious neutral emissions by 2050.<sup>16</sup> To fully realise the success of greenhouse gas mitigation strategies in an urban setting, it is essential to have a comprehensive knowledge of the sources and sinks of greenhouse gases at the urban scale. Although the primary target for mitigation will be carbon dioxide, the role of other important greenhouse gases (e.g. methane and N<sub>2</sub>O) cannot be ignored.

The first comprehensive greenhouse gas inventory for HCMC for 2013–2015 was performed in 2017 and reported that the transportation and stationary energy sectors were the dominant anthropogenic greenhouse gas emission sectors, responsible for 45% and 46% of emissions, respectively; emissions from manufacturing industries (46%) and residential buildings (33%) made up the bulk of the emissions from the stationary energy sector.<sup>17</sup> In 2021, a comparable emission inventory was published using satellite-derived urban land use data, detailed activity data and local emission factors for HCMC to develop a second 'bottom-up' emission inventory for 2009–2016 and also identified transport and the stationary energy sector (*i.e.*, manufacturing industry and residential buildings) as the dominant greenhouse gas emission sources.<sup>18</sup> Although dominated by CO<sub>2</sub>, an emission of 0.332 Gg per year for N<sub>2</sub>O was estimated for 2016, having approximately doubled since 2009, reflecting rapid urban expansion. The transportation sector dominated anthropogenic N<sub>2</sub>O emissions, accounting for 0.29 Gg per year in 2016, with motorcycles accounting for approximately three quarters of the emissions, with personal cars responsible for most of the remaining emissions. For the same year, emissions of N<sub>2</sub>O from manufacturing industries and residential buildings were 0.03 Gg per year and 0.01 Gg per year, respectively. However, it is important to stress that many other sources of N<sub>2</sub>O exist within an urban environment, both anthropogenic and natural. Despite this, there remains a lack of *in situ* observations of N<sub>2</sub>O in urban environments in Southeast Asia. Consequently, there remain several research gaps that need to be filled before a comprehensive inventory of all N<sub>2</sub>O sources within HCMC can be compiled. For example, potential sources include wastewater treatment,<sup>19,20</sup> influx from agricultural activities such as rice cultivation in the surrounding region,<sup>21</sup> rivers,<sup>22</sup> hospitals,<sup>23</sup> small contributions from urban green landscape,<sup>24</sup> and from recreational use.<sup>25,26</sup> The identification and quantification of these sources is very difficult due to the large spatial and/or temporal variability of emissions, but it is essential to better understand these emissions to fully



understand how they can be reduced by future mitigation strategies.

From October 2018 to March 2019, instrumentation was deployed in HCMC, Vietnam, to make the first *in situ* measurement of urban N<sub>2</sub>O mole fractions to investigate how *in situ* atmospheric observations could help to characterise sources of N<sub>2</sub>O in HCMS. This activity was part of a larger project focusing on air pollution sources in HCMC and Hanoi.<sup>27–29</sup> This study addresses several research gaps in our current understanding of urban emissions in HCMC through the implementation of *in situ* observations, characterisation of N<sub>2</sub>O diurnal cycles, identification of important emission sources and quantification of an underexplored anthropogenic source of N<sub>2</sub>O, namely recreational use. The use of N<sub>2</sub>O for recreational purposes has raised serious health concerns globally, as it has been reported that N<sub>2</sub>O abuse can lead to several neurological conditions, and even death.<sup>30–32</sup> Recently, concern has been raised regarding the increased use of N<sub>2</sub>O in China, where it is considered an emerging public health problem<sup>33,34</sup> and in Southeast Asia, including Vietnam.<sup>35</sup> Despite this, no comprehensive data exist regarding the prevalence and demographics of N<sub>2</sub>O use in Vietnam. In 2019, the Vietnamese Ministry of Health approved a request by the Hanoi administration to ban the recreational use of N<sub>2</sub>O due to its harmful effects on human health, thus making it illegal to supply N<sub>2</sub>O for recreational use within Hanoi, Vietnam's second-most populous city. However, despite the ban, it has still been sold openly in bars and restaurants in large cities in Vietnam, such as those on the Bùi Viện Walking Street in HCMC, until new national legislation came into force in 2025 to enforce the ban by decree.<sup>36</sup> Although signals from recreational use of N<sub>2</sub>O have recently been reported for urban areas,<sup>25,26</sup> to the best of our knowledge, this is the first time that an atmospheric signal of this magnitude has been attributable to the recreational use of N<sub>2</sub>O. This source has the potential to be important in greenhouse gas mitigation policies within the city and potentially other large megacities where the recreational use of N<sub>2</sub>O is common.

## 2. Materials and methods

### 2.1. Study site and background information

Continuous *in situ* mole fractions of N<sub>2</sub>O and carbon monoxide were made from the roof of an 11-storey building (~40 m) at the Vietnam National University HCMC, University of Science campus (10.7625°N, 106.6823°E) (Fig. 1). The building is situated in a densely populated central district characterized by mixed residential, commercial, and educational areas with several major urban roads. Given the elevation of the measurement site, it captures the influence of various mixed anthropogenic and natural urban sources, including domestic and commercial emissions, at different magnitudes throughout the day, depending on boundary layer dynamics. During the day, this location can be considered representative of the city's broader urban emission characteristics, rather than a site dominated by local traffic. However, at night, it is expected that the emission footprint will be strongly influenced by local emissions. The instrumentation was housed in a purpose-built,

air-conditioned laboratory situated on the roof. Throughout HCMC the traffic is frequently congested between 6:00 a.m. to 10:00 p.m. every day of the week and is dominated by motorcycles, which account for an estimated 8 million vehicles.<sup>28,37</sup>

### 2.2. Continuous observations of N<sub>2</sub>O and CO mole fractions

Nitrous oxide and carbon monoxide mole fractions were measured using Integrated Cavity Output Spectroscopy (ICOS), Los Gatos Research, model N<sub>2</sub>O/CO-23d. Sampled air for *in situ* analysis of N<sub>2</sub>O and CO mole fractions was drawn from the top of a 15 m telescopic mast through  $\frac{1}{4}$  Synflex® tubing and dried using a Nafion™ membrane in reflux mode before entering the analyser. The analyser was calibrated every 23 hours with gas reference standards prepared at the Max Plank Institute for Biogeochemistry GasLab and is traceable to World Meteorological Organisation (WMO) internationally recognised calibration scales, namely WMO X2006A and WMO X2014A for N<sub>2</sub>O and CO, respectively. Analyser output was corrected for instrumental drift between calibrations using a working reference cylinder, consisting of dry ambient air, which was introduced to the analyser every 6 hours. Calibration and drift corrections were applied instantaneously to the analyser output using bespoke software designed at the University of East Anglia. This software took the analyser output and calculated how much the instrument response changed for a constant sample (e.g., working reference, calibration gas); as this change was a result of a drift in the instrument response, and not a real change in what is being measured, any offsets were used to rescale the instrument output; a full version of this software is available at Github (<https://github.com/UEA-envsoft/GGA-Calculations.git>) and an expanded description of how it works is given in the supplement. The analyser used in this study is over 15 years old, and this was particularly evident in the reduced precision of the instrument when compared with the performance of later models using ICOS technology. This reduced precision was a combination of degraded optics in the analyser and the reduced precision associated with older models of ICOS analysers. To achieve a precision and accuracy suitable for this study, 1-Hz measurements from the working reference gas were averaged over 5 minutes to achieve a precision better than  $\pm 0.5$  nmol mol<sup>-1</sup> for N<sub>2</sub>O and  $\pm 5$  nmol mol<sup>-1</sup> for CO. It is noted that these precisions would not be suitable for observations in rural or remote regions where WMO precision goals would be desirable. However, the reduced precision was sufficient as the deviations from 'background' mole fractions were several orders of magnitude above this WMO precision goal. During the continuous observations, the N<sub>2</sub>O and CO mole fractions were often above the calibrated range of the reference gas standards (324.4–345.2 nmol mol<sup>-1</sup> for N<sub>2</sub>O and 103.3–509.8 nmol mol<sup>-1</sup> for CO). Furthermore, in many instances, the mole fractions were higher than the upper limits of the WMO X2006A scale for N<sub>2</sub>O and the WMO X2014A for CO, where the upper limits are approximately 370 nmol mol<sup>-1</sup> and 500 nmol mol<sup>-1</sup>, respectively.<sup>38</sup> The linearity of the N<sub>2</sub>O/CO-23d is explored in the next section to assess the impacts on uncertainty.



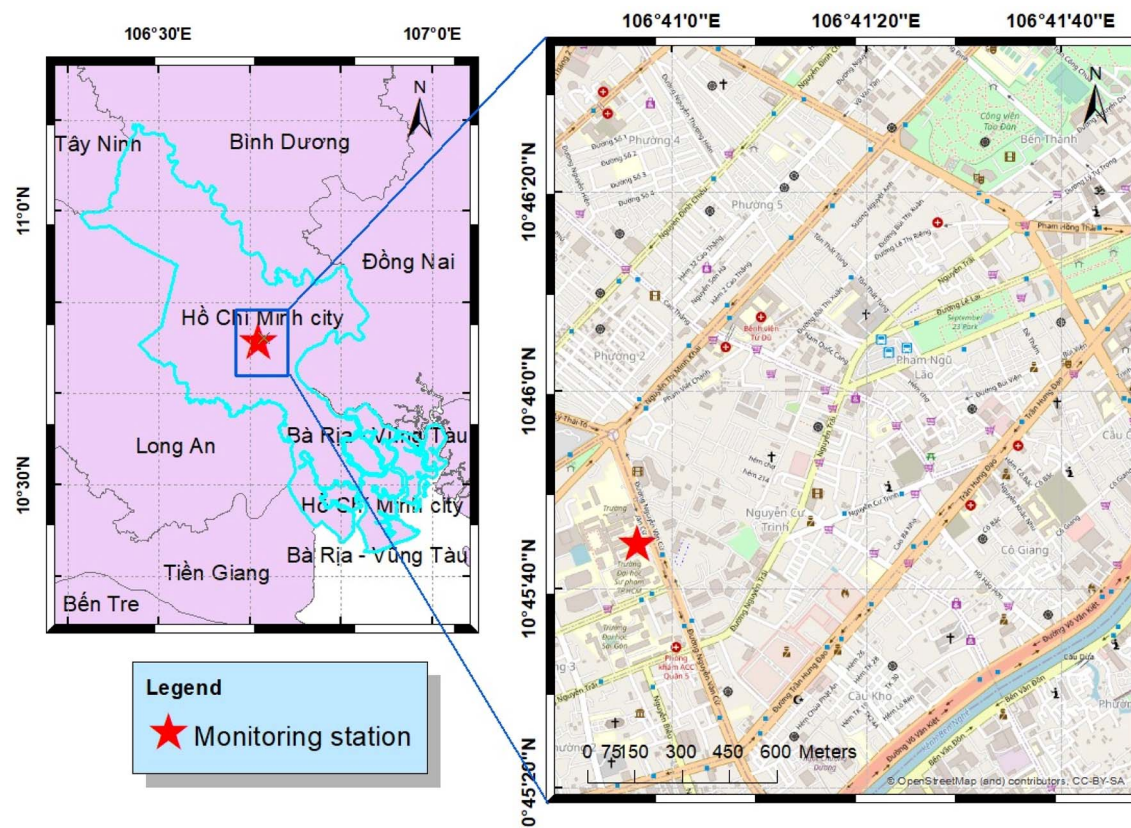


Fig. 1 Sampling site in Ho Chi Minh City. The right panel represents an exploded view of the blue rectangle in the left panel.

### 2.3. Analyser linearity tests for continuous observations of $\text{N}_2\text{O}$

As the upper limits of the *in situ*  $\text{N}_2\text{O}$  observations were above the calibrated range of the instrument, an extrapolation of the linear fit generated from the reference gases was used to assign mole fractions to observations exceeding 345.2 nmol mol<sup>-1</sup>. To test the accuracy of this linear extrapolation, a post-campaign linearity test was performed on the analyser to assess its linearity up to approximately 750 nmol mol<sup>-1</sup> of  $\text{N}_2\text{O}$ . This test was performed using 2 Mass Flow Controllers (MFCs, Alicat Scientific, 0–500 SCCM, accuracy  $\pm 0.6\%$  of reading or 0.1% full scale) to dilute a high  $\text{N}_2\text{O}$  mixture with 'N<sub>2</sub>O-free' air. The high  $\text{N}_2\text{O}$  mixture of approximately 40 000 nmol mol<sup>-1</sup>, was prepared at the University of East Anglia Cylinder Filling Facility in a 5 L aluminium cylinder (Luxfer). Although the exact mole fraction in the mixture was unknown, this did not affect the test, as it was diluted down to a range where the analyser was reporting mole fractions in the required range. Each prepared dilution was run through the analyser for 15 minutes, and the 1-Hz data was averaged over the last 10 minutes. Fig. 2 shows that the analyser was linear for the range of the continuous observations. It is important to note that any residuals observed in Fig. 2 are a result of analyser precision and the uncertainty in the certification of the MFCs used for dilution. As a linear correction was used to calculate mole fractions, as described in Section 2.2, it was felt that confirming the linearity of the

uncalibrated analyser response was sufficient to confirm the linear nature of the analyser's response for the mole fraction range that was observed in the *in situ* measurement. However, these tests revealed a mole fraction dependence on the precision ( $\pm 1\sigma$  standard deviation) of the 1 Hz measurements;  $\pm 0.5$  nmol mol<sup>-1</sup> at 333 nmol mol<sup>-1</sup>, and  $\pm 1$  nmol mol<sup>-1</sup> at 739 nmol mol<sup>-1</sup> ( $y = 0.0012x + 0.1412$ , where  $y$  is the 1 sigma standard deviation of the 1-Hz data and  $x$  is the  $\text{N}_2\text{O}$  mole fraction in nmol mol<sup>-1</sup>,  $R^2 = 0.9823$ ). In conclusion, the precision of the *in situ* observations is better presented as 0.15% of the mole fraction, rather than defining the precision in nmol mol<sup>-1</sup>.

### 2.4. Discrete sampling for $\text{N}_2\text{O}$ mole fraction

Samples for 'discrete' analysis of  $\text{N}_2\text{O}$  mole fractions were collected with Tedlar bags (4 L, SKC Ltd) and were stored in the dark and analysed within 12 hours of being collected. Each Tedlar bag was introduced to the ICOS analyser (see Section 2.2) upstream of the Nafion™ membrane, and the 1 Hz data from the analyser was averaged over 5 minutes. To determine the  $\text{N}_2\text{O}$  mole fractions from the 'discrete' samples in the field, an extrapolation of the linear fit through the calibration gases was applied. Unexpectedly, the  $\text{N}_2\text{O}$  mole fractions recorded by the analyser were up to approximately 2 orders of magnitude higher than the calibrated range. Therefore, post campaign, a further linearity test was performed on the analyser for this higher



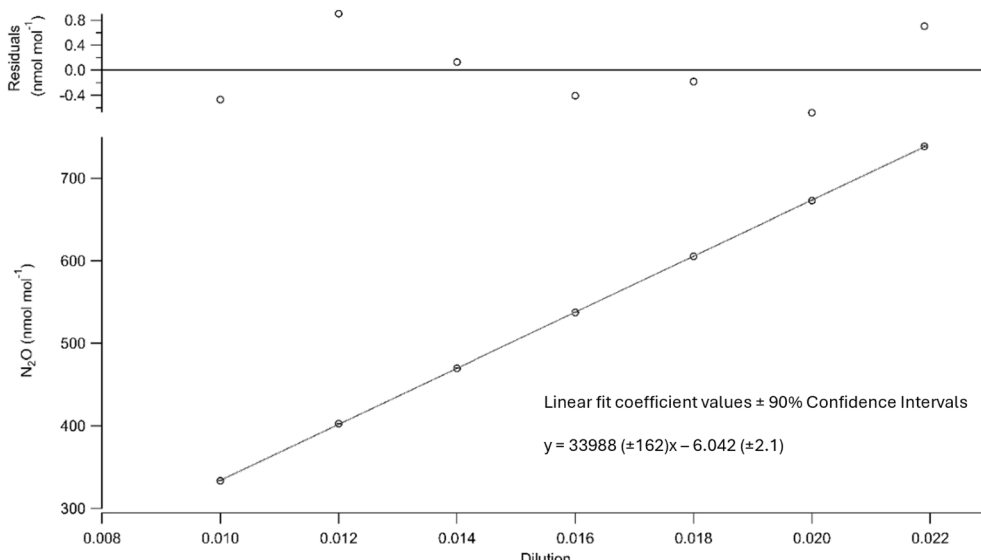


**Fig. 2** Results of linearity test for N<sub>2</sub>O/CO-23d. The top panel shows the residuals of the fit shown in the bottom panel. The x-axis represents the percentage of the flow that is made up of the high concentration standard, with the remainder being 'N<sub>2</sub>O-free' air.

range following the same protocol described in Section 2.3. These tests demonstrate that the analyser was sufficiently linear for the amount fraction range measured during the 'discrete' sampling (Fig. S1). It is difficult to assess the overall uncertainty of these observations as a function of instrument linearity, as a certified N<sub>2</sub>O standard in the higher range was not available. Furthermore, potential storage effects on N<sub>2</sub>O mole fraction likely exceed any uncertainties arising from instrument linearity. A study investigating the effects of storage on N<sub>2</sub>O mole fractions in Tedlar bags highlighted that significant amounts of N<sub>2</sub>O (15.2%) can be lost over 10 days, with higher losses in more humid atmospheres. This represents an approximate loss rate of 1.5% per day and, assuming the loss is linear, would result in approximately 0.75% loss during 12 hours of storage. As the nature of the loss is not characterised in Silva *et al.*,<sup>39</sup> and this represents the dominant uncertainty in the analysis, a conservative estimate of  $\pm 2\%$  uncertainty for the mole fractions reported for the 'discrete' analysis was applied. It is important to stress that the 'discrete' observations were used exclusively to identify N<sub>2</sub>O 'hotspots', and the accurate determination of the uncertainty at these higher mole fractions is not crucial to the interpretation. Therefore, these effectively identify the N<sub>2</sub>O 'hotspot' on the Bùi Viện Walking Street. However, it is important to stress that it is not recommended that these observations be used for quantitative analysis and that extensive characterisation of instrument response up to approximately 30 nmol mol<sup>-1</sup> would be needed for accurate observations. Furthermore, a comprehensive test would need to be performed to establish the characteristics of N<sub>2</sub>O loss in Tedlar bags to account for storage effects.

## 2.5. Meteorology

The wind speed and wind direction were measured using a 2-axis ultrasonic wind sensor (WindSonic, Gill Instruments Ltd)

located at the top of the 15 m mast and recorded every minute *via* a bespoke logging system supplied by the UK National Centre for Atmospheric Sciences (NCAS). Additional observations for wind speed and wind direction were obtained from Ho Chi Minh City International Airport through WeatherOnline Ltd (<https://www.weatheronline.co.uk/>).

## 2.6. ADMS-Urban model description and setup

ADMS-Urban, developed by Cambridge Environmental Research Consultants (CERC), was used to simulate N<sub>2</sub>O at the measurement site for the entire data period shown in Fig. 3. ADMS-Urban is a quasi-Gaussian pollution dispersion and chemistry model that has been applied worldwide for environmental regulation, investigation and assessment of emission control strategies and the generation of high spatial resolution air quality forecasts. In the model, pollutant emissions can be represented as individual plumes dispersing from a range of explicitly represented sources, including point, road, area, and volume sources. For this study, N<sub>2</sub>O emissions from Bùi Viện Walking Street are modelled as a 2D area source. Plume dispersion calculations are driven by vertical flow field and turbulence profiles derived from a single set of meteorological observations representative of upwind conditions and assumed to be constant across the modelled area. Here, temperature and wind speed/direction measured at the airport were used, and cloud cover was approximated as a constant 4 oktas. These upwind profiles are displaced in the model through distinct definitions of surface roughness ( $Z_0$ ) and minimum Monin-Obukhov length ( $L_{MO}$ ) at the airport meteorological site ( $Z_0 = 0.5$  m and  $L_{MO} = 30$  m) and across the built-up urban modelling domain ( $Z_0 = 1.5$  m and  $L_{MO} = 100$  m) to account for the impact of the urban fabric and morphology on atmospheric stability. This model configuration was chosen based on a previous application of ADMS-Urban for a similarly built-up urban



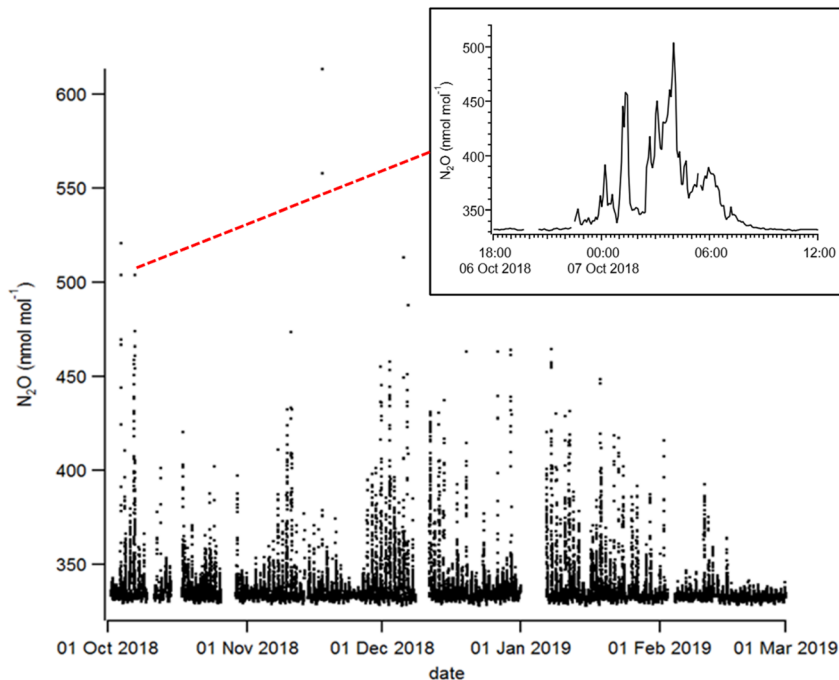


Fig. 3 Time series of  $\text{N}_2\text{O}$  mole fractions (5-minute averages) from HCMC University site from the 1st of October 2018 until the 1st of March 2019. The Inset panel shows overnight observations from the 6th–8th of October 2018. Data gaps in the time series represent periods when the instrument was not operating.

environment in Beijing, China.<sup>40</sup> The local emission of  $\text{N}_2\text{O}$  adds to background pollutant mole fractions representing the underlying regional pollution levels. As there was only a single measurement site for this study, the daily minimum measured  $\text{N}_2\text{O}$  mole fraction was used as a constant background for every 24 hours. Usually, the chemical transformation of pollutants contained within each dispersing plume is represented using the GRS chemistry scheme (including  $\text{NO}_x$ ,  $\text{O}_3$  and VOCs); however, herein,  $\text{N}_2\text{O}$  is released passively as the only emitted gas, so no chemistry is taking place. Emissions from Bùi Viện Walking Street occur constantly between 9:00 p.m.–5:00 a.m. (the mass from the equivalent of 1000, 3000, 5000 or 7000 balloons was spread evenly over this period, released from a height of 1.5 m). Modelled mole fractions are output at the sampling site located at a height of 40 m (approximately the top of the building).

### 3. Results

#### 3.1. $\text{N}_2\text{O}$ time-series

Fig. 3 shows the time series of 5-minute-averaged  $\text{N}_2\text{O}$  mole fractions measured in HCMC from the 1st of October 2018 until the 1st of March 2019. The period was dominated by frequent periods of elevated mole fractions of  $\text{N}_2\text{O}$ , typically more than  $350 \text{ nmol mol}^{-1}$ , lasting for several hours (see Fig. 3 inset) and often elevated above  $400 \text{ nmol mol}^{-1}$  with a maximum of  $613 \pm 0.9 \text{ nmol mol}^{-1}$  measured on the 18th of November at 1:45 a.m. Throughout the measurement period, the mean  $\text{N}_2\text{O}$  mole fraction was  $335.4 \pm 9.7 \text{ nmol mol}^{-1}$  (1-sigma standard deviation), with the 10th and 90th percentiles of  $330.8 \pm 0.5 \text{ nmol mol}^{-1}$

$\text{mol}^{-1}$  and  $340.3 \pm 0.5 \text{ nmol mol}^{-1}$ , respectively. The mean mole fraction during the day between 12:00–14:00 local time (*i.e.*, representing the well-mixed atmosphere) was  $332.25 \pm 1.05 \text{ nmol mol}^{-1}$  ( $\pm 1\sigma$  standard deviation), which is in close agreement with the monthly average of  $331.97 \pm 0.76 \text{ nmol mol}^{-1}$  at Mauna Loa ( $19.539^\circ\text{N}$ ,  $155.578^\circ\text{W}$ ) for December 2018.<sup>41</sup>

#### 3.2. Diurnal pattern and wind dependence

The mean diurnal cycle of  $\text{N}_2\text{O}$  (and  $\text{CO}$ ) mole fractions throughout the measurement period for the different wind sectors is shown in Fig. 4. The diurnal variation in the  $\text{N}_2\text{O}$  mole fractions throughout the measurement period was consistent with what would be expected from the dynamics associated with atmospheric boundary layer mixing (see Fig. S2 and S3 in SI). This agrees well with the boundary layer height from ERA5 global climate reanalysis<sup>42</sup> produced by the Copernicus Climate Change Service (C3S) and the European Centre for Medium-Range Weather Forecasts (ECMWF) for the  $0.25^\circ \times 0.25^\circ$  grid cell in which the *in situ* observation was made. The  $\text{N}_2\text{O}$  mole fractions in all wind sectors were higher between 6:00 p.m. and 6:00 a.m. every evening, coincident with shallower mixing heights (Fig. S4). Although the diurnal pattern was consistent for the different wind sectors, the amplitude of the diurnal cycle varied. The southeast through north wind sectors display elevations during the evening in the range of  $5\text{--}10 \text{ nmol mol}^{-1}$  when compared with the mole fractions measured in the afternoon. The largest enhancements (above  $50 \text{ nmol mol}^{-1}$ ) occurred in air arriving from the northeast and east. Fig. 5



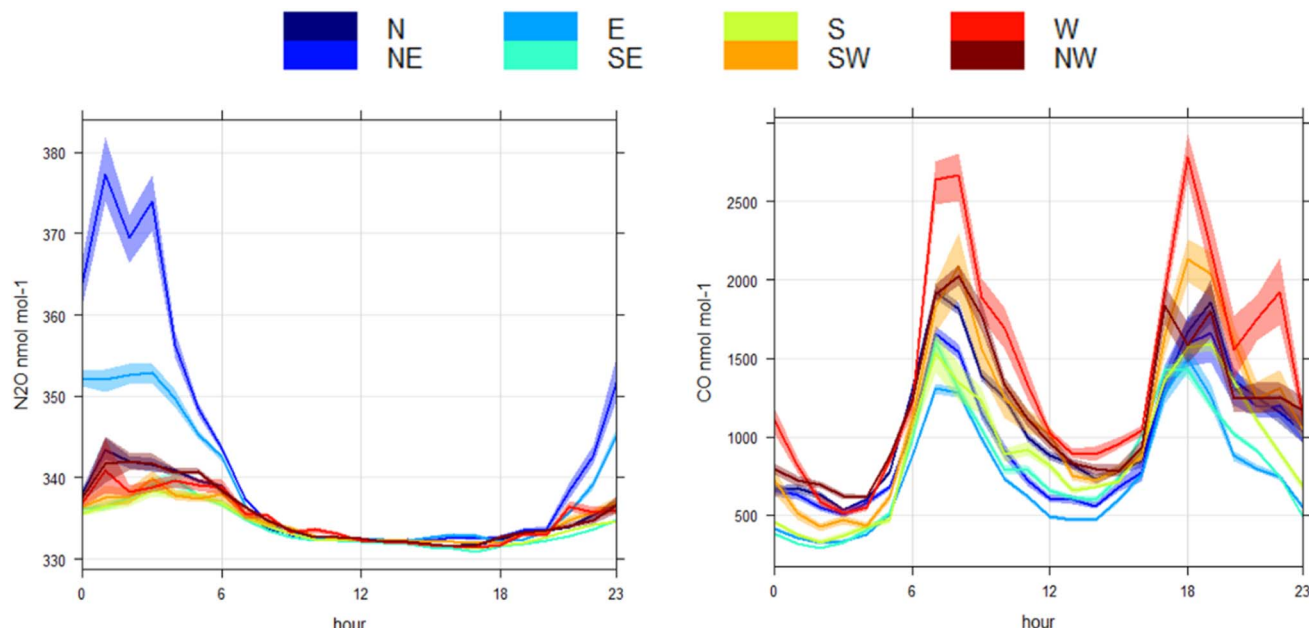


Fig. 4 Diurnal cycles of  $\text{N}_2\text{O}$  mole fractions (left panel) and CO mole fractions (right panel) by wind sector for the period 1st of October 2018 to 1st of March 2019. Shaded areas represent the 90% confidence interval in the mean. Generated in Openair (Carlslaw, 2019).

shows a Conditional Probability Function (CPF) plot, generated using Openair,<sup>43</sup> to show the probability of high mole fractions occurring in certain wind directions.<sup>44</sup> It is clear from this plot that the observations above the 90th percentile ( $340.3 \text{ nmol mol}^{-1}$ ) for the *in situ*  $\text{N}_2\text{O}$  observations are predominantly associated with air arriving from the northeast and east with a probability between 0.21–0.31. These large elevations in  $\text{N}_2\text{O}$  mole fractions shown in Fig. 3 coincided with low wind speeds of  $2.0 \pm 1.2 \text{ m s}^{-1}$  ( $\pm 1\sigma$  standard deviation) and air arriving from the northeast and east between 6:00 p.m. and 6:00 a.m. (Fig. 4).

As it is well recognised that traffic can be an important source of  $\text{N}_2\text{O}$  in the urban environment,<sup>45,46</sup> the correlation

between excess  $\text{N}_2\text{O}$  and CO was calculated ( $\text{N}_2\text{O}/\text{CO}$  ratio) to see if there was a measurable relationship between  $\text{N}_2\text{O}$  and CO emissions traffic in HCMC. To isolate the traffic peak that dominates the CO profile from late afternoon until early evening (15:00–18:00), data were filtered to exclude any data outside of this time. This peak was chosen as the morning traffic peak was heavily influenced by the overnight  $\text{N}_2\text{O}$  emissions. Data were further filtered to remove any influence of  $\text{N}_2\text{O}$  arriving from the northeast and east by removing data that was coincident with wind bearing  $337.5^\circ$  through  $112.5^\circ$ . Finally,  $\text{N}_2\text{O}$  and CO mole fractions were converted to excess mole fraction by subtracting the average between 12:00–14:00 to represent air that was well mixed;  $332.25 \text{ nmol mol}^{-1}$  and

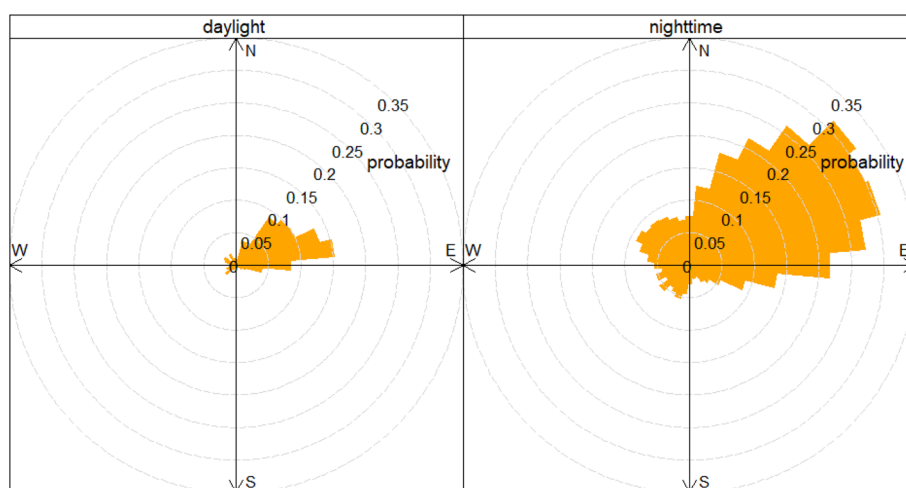


Fig. 5 Conditional probability function for periods when  $\text{N}_2\text{O}$  was above the 90th percentile split by daylight (left panel) and nighttime (right panel). The radial axis represents the probability that air arriving from a specific direction will have  $\text{N}_2\text{O}$  mole fractions above the 90th percentile ( $340.3 \text{ nmol mol}^{-1}$ ). Generated in Openair (Carlslaw, 2019).



681.80 nmol mol<sup>-1</sup> for N<sub>2</sub>O and CO, respectively. The resulting correlation between excess N<sub>2</sub>O and excess CO was low ( $R^2 = 0.0004$ ), giving an excess N<sub>2</sub>O/CO (*i.e.* slope) ratio of 0.00004. This suggests that the *in situ* observations presented herein cannot effectively capture N<sub>2</sub>O/CO ratios for the traffic fleet associated with the increases in CO during the day. The potential implications and reasons for this are discussed in more detail in Section 4.4.

### 3.3. Discrete sampling to identify a strong local source of N<sub>2</sub>O

To further investigate the large elevations in N<sub>2</sub>O in air arriving from the northeast and east, random 'discrete' sampling was carried out in the area to the northeast of the observation site to identify potential 'hotspots' of elevated N<sub>2</sub>O mole fractions on the evening of 16th of March 2019 (see Fig. 6). An area with enhanced N<sub>2</sub>O mole fractions was identified in Bùi Viện Walking Street and surrounding area which is located approximately 1 km northeast of the measurement site (Fig. 6). Although consistently elevated, N<sub>2</sub>O mole fractions across this area were very heterogeneous with a minimum of  $373 \pm 7.4$  nmol mol<sup>-1</sup> and a maximum of  $26\,400 \pm 528$  nmol mol<sup>-1</sup>. The mean N<sub>2</sub>O mole fraction within this area was 4733 nmol mol<sup>-1</sup> with a median of 1265 nmol mol<sup>-1</sup> ( $n = 8$ ). Observations outside of this area were consistent with the general diurnal pattern of N<sub>2</sub>O and did not highlight any other potential source regions close to the measurement site. Bùi Viện Walking Street is the most crowded entertainment hub in HCMC, and the use of N<sub>2</sub>O for recreational purposes is widespread and well-documented in the local and national news.

### 3.4. Estimates of N<sub>2</sub>O emission

A typical 'bottom-up' emission estimate uses a detailed calculation of the emissions from all the individual sources within an area, which are subsequently aggregated to obtain the total

emissions from the area. In theory, the volume of N<sub>2</sub>O used on the Bùi Viện Walking Street can be calculated from the turnover rate (*i.e.* the number of cylinders supplied and returned), which could be estimated from the supply of the product from the licensed supplier. However, this approach was not possible in Vietnam as the use of N<sub>2</sub>O for recreational activity is not regulated, only its commercial production and sale. In this section, two different techniques were applied to estimate the emission of N<sub>2</sub>O associated with recreational use on the Bùi Viện Walking Street and the surrounding area.

**3.4.1. Quasi 'bottom-up' emission estimates.** As the sale of N<sub>2</sub>O for recreational use in Vietnam is prohibited, it was not possible to get accurate statistics for how much was being emitted from the Bùi Viện Walking Street, as bar owners were not willing to provide information. It is common to see articles in the Vietnamese press that report on the confiscation of materials used in supplying N<sub>2</sub>O and highlight that there is a major problem in the Bùi Viện Walking Street in HCMC.<sup>47</sup> Therefore, to estimate the magnitude of the N<sub>2</sub>O emissions from the Bui Vien Walking Street, a quasi 'bottom-up' approach was used, which was informed by a visual survey to estimate the scale of this activity. This was performed alongside the 'discrete' sampling campaign described in Section 2.4. In many parts of the world (*e.g.* UK), a N<sub>2</sub>O 'party' balloon is filled using a small canister of N<sub>2</sub>O, known as a "whippet", and typically contains 8 grams of N<sub>2</sub>O. In contrast, the 'party' balloons sold on the Bùi Viện Walking Street and surrounding area were filled using compressed gas cylinders containing high-purity N<sub>2</sub>O and were considerably larger (approximate diameter of 0.5 m, see Fig. S5 in SI) than those typically used in the UK. As a result of this larger balloon volume, the amount of N<sub>2</sub>O in a balloon was estimated at  $123 \pm 20$  grams. Although somewhat crude, from repeated visits to the Bùi Viện Walking Street, it was estimated that  $30 \pm 10$  bars were supplying between  $15 \pm 5$  'party' balloons, which equates to approximately  $57.15 \pm 28.40$  kg of

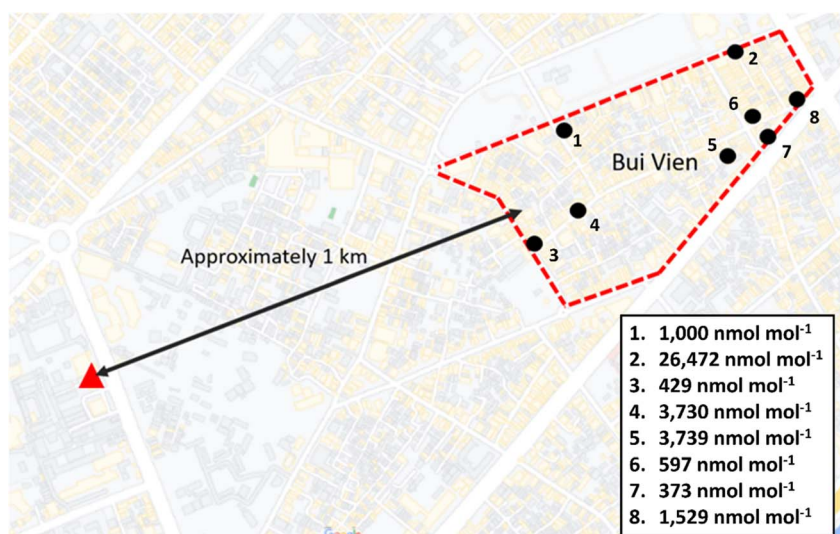


Fig. 6 Map of the study area in HCMC showing the location of the sampling site (red triangle), Bùi Viện Walking Street (red dashed lines) and the 'discrete' sampling locations (black circles). Inset, the mole fraction of N<sub>2</sub>O sampling locations at points 1 through 8.



$\text{N}_2\text{O}$  being emitted to the atmosphere per day. There is a broad consensus within the medical profession that only a very small percentage of the inhaled  $\text{N}_2\text{O}$  (<0.004%) is metabolised in the human body.<sup>48,49</sup> Given that the observations highlight that this increase in  $\text{N}_2\text{O}$  mole fraction from the northeast and east is not limited to certain days of the week (see Fig. S6 in SI), an estimated  $0.021 \pm 0.010 \text{ Gg}$  per year of  $\text{N}_2\text{O}$  could be released from recreational use in the Bùi Viện Walking Street and the surrounding area; a figure that is in the same order as magnitude as the emissions from the stationary energy sector ( $0.03 \text{ Gg}$  per year).<sup>18</sup>

**3.4.2. Estimating  $\text{N}_2\text{O}$  emissions using ADMS-Urban.** In this section, the ADMS-Urban model was used to estimate the emissions of  $\text{N}_2\text{O}$  from the Bùi Viện Walking Street and the surrounding area (for model setup details, see Section 2.6). Fig. 7 shows the diurnal pattern of the observed  $\text{N}_2\text{O}$  mole fractions *versus* the modelled  $\text{N}_2\text{O}$  mole fractions from ADMS-Urban for each wind sector. For this comparison, the average diurnal variation in  $\text{N}_2\text{O}$  mole fractions for the sectors south through west was calculated and added to the model output mole fractions. This was to account for the fact that the model released emissions on top of a stable background of  $\text{N}_2\text{O}$ , and the only emission in the model was from the Bùi Viện Walking Street and the surrounding area. This diurnal variation had a magnitude of approximately  $10 \text{ nmol mol}^{-1}$  (see Section 3.2). If this is considered for the data presented in Fig. 7, a reasonable qualitative agreement between the modelled and observed diurnal profile structure for the northeast sector is apparent and consistent with the existence of a strong source of  $\text{N}_2\text{O}$  located in the vicinity of the Bùi Viện Walking Street. This represents an emission of  $1016 \text{ kg N}_2\text{O}$  each evening between 9:00 p.m.–5:00 a.m., which is equivalent to the mass of  $\text{N}_2\text{O}$  that would be released from approximately 7000 'party' balloons. The model

performance was assessed for this level of emission by calculating an Index of Agreement (IOA) in Openair of  $0.402$ .<sup>43</sup> The IOA is a commonly used tool to evaluate model performance against observations,<sup>50</sup> where a value of +1 represents the best model performance. Although consistent with the location of the strong source from the Bùi Viện Walking Street, the emission of  $\text{N}_2\text{O}$  needed to reproduce the observations was over an order of magnitude higher than the estimate using the 'bottom-up' approach in Section 3.4.1. It is important to note that the mismatch between the simulated and 'bottom-up' emission estimates likely result from a combination of poorly simulated advection of the emissions from the Bùi Viện Walking Street to the measurement site and from an underestimation of emissions using the 'bottom-up' accounting. To illustrate the potential mismatch caused by poorly represented advection, Fig. 8 shows a cross-section of the model at 1:00 a.m. on the 7th of December 2018. This clearly shows that modelled plume maxima (approximately  $420 \text{ nmol mol}^{-1}$ ) did not reach the measurement site and offers a potential explanation as to why such high emissions from the Bùi Viện Walking Street were needed to simulate the mole fractions measured at the observation site. Additionally, our approach of uniformly distributing the emissions across the Bùi Viện Walking Street may not be an appropriate strategy given the large heterogeneity observed during the discrete sampling.

## 4. Discussion

### 4.1. $\text{N}_2\text{O}$ from catalytic converters and unknown sources in HCMC

In contrast with  $\text{N}_2\text{O}$ , the diurnal pattern in CO mole fractions had two distinct peaks coincident with morning and evening traffic counts and daily atmospheric boundary layer mixing

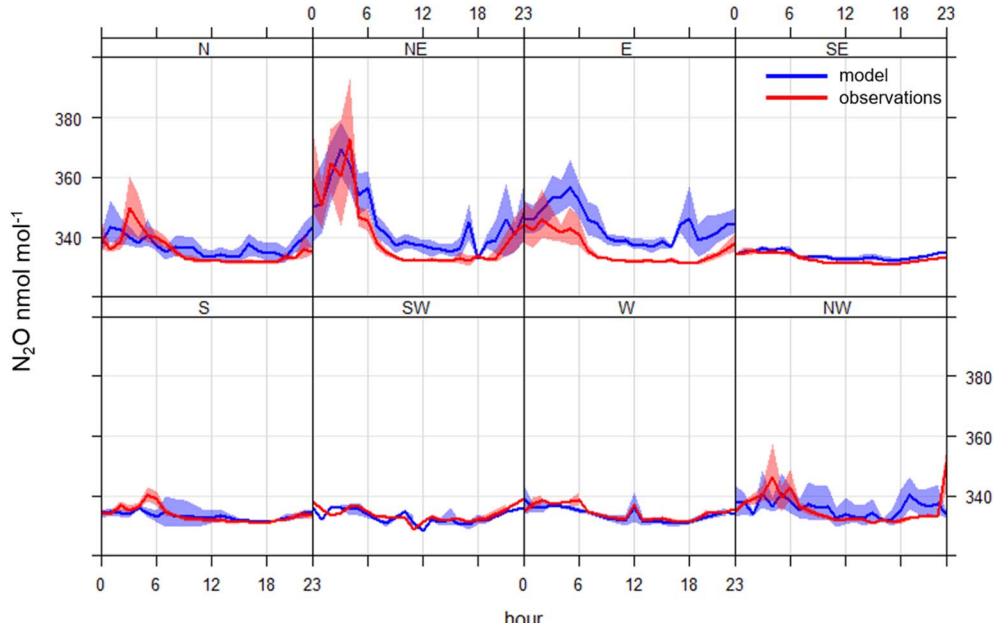


Fig. 7 Modelled  $\text{N}_2\text{O}$  mole fractions *versus* observed  $\text{N}_2\text{O}$  mole fractions for the entire dataset. The modelled results are superimposed upon the mean diurnal cycle from the southwest sector as calculated from the observations. Generated in Openair (Carlslaw, 2019).



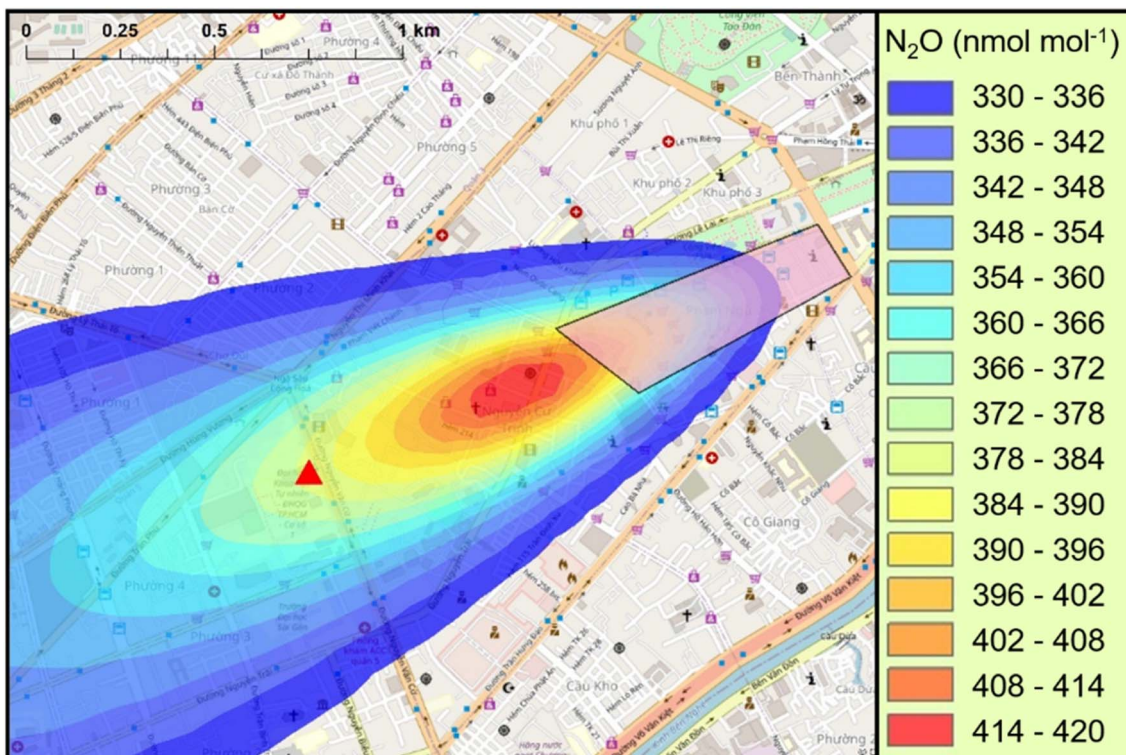


Fig. 8 Vertical slice of the ADMS-Urban model output showing  $\text{N}_2\text{O}$  mole fractions at 40 m at 1 a.m. on the 7th of December 2018. The red triangle represents the measurement location, and the pink trapezoid represents the area for which  $\text{N}_2\text{O}$  emissions were added in the ADMS-Urban model.

(Fig. 4). This diurnal pattern was consistent across all wind sectors with varying amplitude. The lowest elevations in carbon monoxide were associated with air coming from the east, and the highest elevations were associated with air coming from the west. This can be explained by the location of the sampling site, as district 5 is bordered on the east by a region with a lower traffic density. Whereas the air arriving from the west would have passed through the more densely populated urban districts and may have collected increased traffic emissions en route to the observation site.

The underlying diurnal pattern of higher  $\text{N}_2\text{O}$  mole fractions at night in all sectors was likely dominated by emissions from the transportation sector, given its dominant role in published inventories.<sup>18</sup> It is important to note that the vehicular fleet mix transitions at night with an influx of heavy diesel trucks from 10:00 p.m. to 6:00 a.m. (Fig. S7).<sup>37</sup> Therefore, despite significantly lower numbers of vehicles at night, it is probable that a significant portion of  $\text{N}_2\text{O}$  associated with transportation was from heavy trucks fitted with three-way catalytic converters (TWC), as the molar ratio of  $\text{N}_2\text{O}/\text{CO}$  emitted from vehicles with TWC can be several orders of magnitude higher than vehicles without.<sup>51,52</sup> However, it is unlikely that this could have been the sole cause of increased  $\text{N}_2\text{O}$  mole fractions in air arriving from the northeast and east (*i.e.* strong local source) as these vehicles would be operating predominantly to the west and north of the sampling site. In addition to the large source of  $\text{N}_2\text{O}$  from traffic, the second largest anthropogenic source of  $\text{N}_2\text{O}$  in

HCMC is from the stationary energy sector and will form a component of nighttime emissions, although emissions from this sector are approximately an order of magnitude lower than for transportation.<sup>17,18</sup> Furthermore, many other potential anthropogenic and natural sources of  $\text{N}_2\text{O}$  can impact HCMC including wastewater treatment,<sup>19,20</sup> influx from agricultural activities such as rice cultivation in the surrounding region,<sup>21</sup> emission from rivers (*e.g.* ref. 22,53 and 54), hospitals,<sup>23</sup> small contributions from urban green urban landscape<sup>24</sup> and from recreational use.<sup>25,26</sup> However, it is beyond the capability of these observations to speculate further on the urban sources of  $\text{N}_2\text{O}$ , which appear to be responsible for the underlying diurnal cycle. Understanding this further would require a substantial increase in the spatial coverage of observations across the city to help identify emission hotspots. In addition, measuring the stable isotopic composition of  $\text{N}_2\text{O}$  would prove to be a valuable tool to identify the processes that are contributing towards the accumulation of  $\text{N}_2\text{O}$  observed for all wind sectors and should be considered in any future work.<sup>55</sup>

#### 4.2. Estimating the emission of $\text{N}_2\text{O}$ from recreational use in HCMC

Despite the localised source of  $\text{N}_2\text{O}$  in the Bùi Viện Walking Street, this study could not quantify  $\text{N}_2\text{O}$  emissions from a single fixed point measurement site, and estimates range from  $57.15 \pm 28.40$  kg per day from 'bottom-up' estimates to 1016 kg per day from the ADMS modelling. The estimate using the



'bottom-up' approach is perhaps modest and could potentially be significantly higher, whereas the emissions in ADMS-Urban required to simulate the observations are extremely high. This suggests that either the 'bottom-up' approach is underestimating emissions, or more likely, the ADMS-Urban setup chosen was not suitable to accurately represent the scenario for the Bùi Viện Walking Street. It is important to stress that the model can reasonably capture the diurnal pattern for each sector and supports the hypothesis that the Bùi Viện Walking Street is a strong source of  $\text{N}_2\text{O}$  in HCMC. The apparent overestimation of emissions using ADMS-Urban could be due to several factors, including poorly captured advection, poor representation of street morphology or assumptions made regarding source distribution.

Evidence supporting misrepresented advection with our setup was presented in Section 3.4.2 with a horizontal cross-section of the model output showing the simulated plume maxima is a considerable distance upwind ( $\sim 300$  m) of the *in situ* measurement site. There are various parameters in the ADMS model which could result in suppressed advection. For example, the boundary layer stability calculated in the model is largely dependent on the cloud cover values used; assuming a constant value of 4 oktas, in the absence of available observations, may be an overestimation for this time of year in HCMC. If a lower value were instead used, the incoming solar radiation calculated by the model reaching the ground surface would increase. This increased surface heating would result in enhanced turbulent mixing and more favourable conditions for the dispersion of the modelled plume towards the observation point.

The effect of street canyons on the dispersion of pollution from the Bùi Viện Walking Street has not been considered in the model setup; however, adding street canyons would likely introduce a further barrier to dispersion, and even higher emissions would be needed to simulate the *in situ* observations. Quantifying the effects of street canyons is very complex and can be influenced by many factors, including building geometry, wind environment, temperature, pollutant type, pavements and building porosity.<sup>56–58</sup> Given that the measured mole fractions are so high at the university, it appears that the street canyons are not proving too much of an obstacle to dispersion.

Finally, the area source that was used in the model assumes that the  $\text{N}_2\text{O}$  emissions are evenly distributed throughout the Bùi Viện Walking Street, but this is not the case, as demonstrated in Section 3.3. The heterogeneous distribution of the source is also demonstrated by the filamentous nature of the mole fraction enhancements observed at the University, as demonstrated in Fig. 3. This represents a further limitation of the modelling work and could lead to an overestimation of the total number of 'party' balloons required to simulate the observed  $\text{N}_2\text{O}$  mole fractions by not explicitly accounting for emission 'hotspots' from the Bùi Viện Walking Street. An extensive survey of the Bùi Viện Walking Street would be needed to better understand the spatial variability of these emissions. In combination with direct measurements, indirect measurements (e.g., stable isotopes, tracer release experiments, mobile

sensing) could be useful to better understand the source heterogeneity.

The 'bottom-up' emissions estimates could be vastly improved with an intense visual survey in the Bùi Viện Walking Street and surrounding areas: this would involve counting the number of 'party' balloons being used in all the bars for a week or more and repeating this activity at regular intervals (*i.e.*, monthly) to assess how the activity varies throughout the year. However, this would be extremely resource-heavy and would be potentially dangerous given the criminal aspect of supplying  $\text{N}_2\text{O}$  for recreational purposes. With respect to the ADMS modelling, a thorough modelling study, in conjunction with the above-mentioned survey, would need to be performed to better understand the key processes contributing to the apparent overestimation presented herein. Future work should focus on statistically evaluating the agreement between measured and modelled mole fractions over the campaign period to determine how each input parameter influences the agreement between the model and the observations.

Despite the disagreement between the 'bottom-up' and modelling approach presented here, the emissions from the Bùi Viện Walking Street are clearly detected from the *in situ* measurements location. As the use of  $\text{N}_2\text{O}$  as a recreational drug has been banned since January 2025 by decree,<sup>36</sup> our measurements can effectively act as a baseline for which future measurements, from the same location, could be compared. This would prove an effective strategy to assess if the nationwide ban is being successfully enforced in the Bùi Viện Walking Street.

#### 4.3. Wider environmental impact of $\text{N}_2\text{O}$ emissions from recreational use

Based on the 'bottom-up' approach used in section 3.4.1, it is estimated that  $0.021 \pm 0.010$  Gg per year of  $\text{N}_2\text{O}$  could be released from recreational use from the Bùi Viện Walking Street and the surrounding area. To put this into context, the estimated emission of  $\text{N}_2\text{O}$  from the stationary energy sector in HCMC was 0.04 Gg per year in 2016.<sup>18</sup> The upper limit of the estimated emissions from HCMC represents a small fraction of the annual  $\text{N}_2\text{O}$  emissions estimates for Vietnam (less than 0.05% of 112 kt), which is predominantly dominated by emissions from agriculture.<sup>14</sup> However, the use of  $\text{N}_2\text{O}$  as a recreational drug is on the rise in many parts of the world,<sup>59</sup> and with over 80 cities in Vietnam alone, the potential for this to be a significant unregulated source in urban environments is significant. Additionally, the health effects of using  $\text{N}_2\text{O}$  recreationally need to be fully assessed to determine what risks it poses to the Vietnamese population. To be effective, this will require detailed statistics to derive a useful estimate for nationwide emissions and health impacts. For example, Charoenpornpukdee *et al.*<sup>26</sup> derived a UK estimate of  $\text{N}_2\text{O}$  emissions from recreational activity using essential scaling factors, such as the number of users, the frequency of use and the number of instances of use. Nevertheless, this work demonstrates that the emission of  $\text{N}_2\text{O}$  from this activity needs to be included when compiling emission inventories and when implementing



mitigation strategies to fulfil Vietnam's commitments to the UNFCCC by 2050 (*i.e.* Net Zero).

#### 4.4. Important note on N<sub>2</sub>O/CO emission ratios from traffic peaks in urban environments

Previous studies have highlighted the importance of non-agricultural N<sub>2</sub>O emissions in urban environments as a by-product of traffic fossil fuel combustion (*e.g.* road transport) with patterns in the daily variation of N<sub>2</sub>O and traffic counts in correlation.<sup>45,46</sup> Emissions of N<sub>2</sub>O from road traffic in Vietnam have been estimated at 0.23 kt for 2013.<sup>14</sup> For HCMC, Nguyen *et al.*<sup>18</sup> estimate N<sub>2</sub>O from city and emissions of 0.290 Gg for 2016, which represents the major N<sub>2</sub>O emission source in the city, and is nearly an order of magnitude greater than the emissions from the manufacturing industry and construction, and residential emissions combined. It has long been known that the emission of N<sub>2</sub>O from vehicles is predominantly associated with catalytic converters,<sup>52</sup> but estimating urban emissions of N<sub>2</sub>O remains challenging due to a lack of validation data. Given a lack of urban N<sub>2</sub>O observations, it is common for national emission inventory agencies to estimate N<sub>2</sub>O emissions for traffic using excess N<sub>2</sub>O/CO molar ratios of emissions for different vehicle types derived from field and lab-based studies.<sup>45,46,60–63</sup> For example, the UK's National Atmospheric Emission Inventory<sup>51</sup> uses a range from 0.0009 for motorcycles to 0.1142 for large goods vehicles with TWCs (Table 1). Vehicles without three-way TWCs produce only small amounts of N<sub>2</sub>O (*i.e.*, motorcycles), relative to CO, when compared with vehicles fitted with TWCs (*i.e.*, large goods vehicles), typically a couple of orders of magnitude less.<sup>64,65</sup> Given the dominance of the non-catalyst vehicles in HCMC during the day (*i.e.*, motorcycles), N<sub>2</sub>O from the traffic fleet during the day would be hard to detect above<sup>64,65</sup> background N<sub>2</sub>O mole fractions using *in situ* atmospheric observations with a precision of 0.5 nmol mol<sup>−1</sup>. Therefore, the lack of a strong correlation between excess N<sub>2</sub>O and CO for the traffic peaks during this study ( $R^2 = 0.0004$ ) is not unexpected (see Section 3.2) and highlights that care must be taken when estimating N<sub>2</sub>O emissions from traffic using N<sub>2</sub>O/CO ratios derived from this type of atmospheric measurement. Furthermore, it demonstrates that citing atmospheric measurements closer to the traffic sources (*i.e.*, roadside) would be better for deriving N<sub>2</sub>O/CO emission ratios and for validating 'bottom-up' inventories, as it is more likely that N<sub>2</sub>O would be detectable above background mole fractions.

**Table 1** Emission factors for N<sub>2</sub>O/CO for a range of vehicle types operating in an urban environment from the NAEI (2024)

Vehicle type	Molar N <sub>2</sub> O/CO ratio
Petrol cars	0.0023
Diesel cars	0.0540
Petrol LGV's	0.0009
Deisel LGV's	0.1142
Buses	0.0277
Motorcycles	0.0009

#### 4.5. Improving urban measurement networks

This study emphasises how the location of the observations is extremely important when identifying and quantifying urban sources of greenhouse gases and other pollutants. A better understanding of sources of greenhouse gases within cities will require a measurement network to have significant spatial and temporal coverage. Due to cost implications, it is unlikely that this can be achieved using state-of-the-art instrumentation (typically >£100k per instrument for N<sub>2</sub>O), and the implementation of such a network will require advancements in small deployable sensor technology. Such strategies have been effectively deployed in urban environments in other parts of the world for carbon dioxide and air quality-related parameters such as nitrogen dioxides and particulate matter.<sup>66–69</sup> However, obtaining a suitable accuracy and precision for the determination of N<sub>2</sub>O mole fractions using small sensors has proven to be challenging, and the precision of current sensor technology remains a few orders of magnitude too high for their effective deployment in measuring ambient atmospheric mole fractions.<sup>70</sup> An alternate solution is to survey the city using mobile instrumentation as has been demonstrated for methane;<sup>71–74</sup> this would have been useful in identifying the strong source of N<sub>2</sub>O in Section 3.3 and would help us to better understand the spatial variability which could then be accounted for in the ADMS-Urban modelling. Future work should also consider how indirect methods, such as stable isotope analysis and tracer release experiments, could be used to better understand emission sources and to quantify the effects of local meteorology. It is important to note that the location of the observation site in this study was not designed to target the N<sub>2</sub>O emission from recreational use, and it was coincidental that we were close to the source of elevated N<sub>2</sub>O mole fractions. Therefore, this emphasises the important role that dense measurement networks or mobile measurements of greenhouse gases can play in the identification and quantification of urban N<sub>2</sub>O sources.

## 5. Conclusions

The results of this study highlight the important role that *in situ* atmospheric observations of N<sub>2</sub>O mole fractions and other gases can have in identifying sources within an urban environment. Continuous *in situ* observations of atmospheric N<sub>2</sub>O mole fractions were used to identify a strong source of N<sub>2</sub>O associated with recreational activity and estimate emissions using two techniques, a 'bottom-up' approach and a modelling approach. The model could not accurately reproduce the magnitude of the N<sub>2</sub>O mole fractions observed at the measurement site but could capture the diurnal patterns observed for the various wind sectors. This indicated that recreational activity in the Bùi Viện Walking Street is responsible for the elevated N<sub>2</sub>O mole fractions measured overnight in air arriving from the northeast and east. Despite the mismatch in 'bottom-up' *vs.* model emissions estimates, the atmospheric measurements presented herein act as a baseline to assess the effectiveness of a nationwide ban that came into force in 2025.



Furthermore, from the *in situ* observations, it was shown that care must be taken when using field-derived N<sub>2</sub>O/CO molar emission ratios to estimate N<sub>2</sub>O emissions from traffic in megacities where traffic fleets are dominated by motorcycles (*i.e.* a lower proportion of vehicles with catalytic converters). Finally, this study highlights that more observations are needed in urban environments to accurately detect and quantify emissions and suggests how this could be achieved.

## Author contributions

Grant Forster: conceptualisation, analysis, writing, visualisation, and data acquisition. Michael Biggart: ADMS-Urban modelling, analysis, and writing. Ruth Doherty: comments on the manuscript. David Oram: conceptualisation, writing and funding acquisition. Alex Baker: comments on the manuscript. Alex Etchells: data acquisition software. Graham Mills: data acquisition. To Thi Hien: comments on manuscript. Doan Thien Chi: comments on the manuscript. Duong Huu Huy: comments on the manuscript.

## Conflicts of interest

The authors declare that they have no known competing financial interests or personal relationships that could have appeared to influence the work reported in this paper.

## Data availability

The mole fractions of nitrous oxide and carbon monoxide used in this article will be made available *via* the Centre for Environmental Data Analysis (CEDA) upon acceptance of this manuscript. The code for retrieving data from the gas analysers used in this study can be found on a Github repository at <https://github.com/UEA-envsoft/GGA-Calculations.git>.

Supplementary information (SI) is available. See DOI: <https://doi.org/10.1039/d5ea00083a>.

## Acknowledgements

This research was funded by the RCUK (Research Councils UK)-NAFOSTED (Vietnam National Foundation for Science and Technology Development) Newton Fund Research Partnership under grant number NE/P014771/1. The ADMS-Urban modelling activity was supported through a NERC industrial PhD studentship (NE/N007794/1). The authors thank Cambridge Environmental Research Consultants (CERC) for research-level access to ADMS-Urban.

## References

- United Nations Framework Convention on Climate Change (UNFCCC), Paris Agreement, adopted at the, *21st Conference of the Parties (COP 21) in Paris*, 2015.
- M. J. Prather, J. Hsu, N. M. DeLuca, C. H. Jackman, L. D. Oman, A. R. Douglass, *et al.*, Measuring and modeling the lifetime of nitrous oxide including its variability, *J. Geophys. Res.: Atmos.*, 2015, **120**, 5693–5705.
- IPCC, *Climate Change 2021: The Physical Science Basis. Contribution of Working Group I to the Sixth Assessment Report*, Cambridge University Press, Cambridge, UK & New York, NY, USA, 2021, p. 2391.
- X. Lan, K. W. Thoning and E. J. Dlugokencky, *Trends in Globally-Averaged CH<sub>4</sub>, N<sub>2</sub>O, and SF<sub>6</sub> Determined from NOAA Global Monitoring Laboratory Measurements*, Version 2025-12, 2022.
- R. W. Portmann, J. S. Daniel and A. R. Ravishankara, Stratospheric ozone depletion due to nitrous oxide: influences of other gases, *Philos. Trans. R. Soc. Lond. B Biol. Sci.*, 2012, **367**, 1256–1264.
- E. A. Davidson, The contribution of manure and fertilizer nitrogen to atmospheric nitrous oxide since 1860, *Nat. Geosci.*, 2009, **2**, 659–662.
- A. Syakila and C. Kroeze, The global nitrous oxide budget revisited, *Greenhouse Gas Meas. Manage.*, 2011, **1**, 17–26.
- H. Tian, J. Yang, R. Xu, C. Lu, J. G. Canadell, E. A. Davidson, *et al.*, Global soil nitrous oxide emissions since the preindustrial era estimated by an ensemble of terrestrial biosphere models: Magnitude, attribution, and uncertainty, *Global Change Biol.*, 2019, **25**, 640–659.
- H. Tian, R. Xu, J. G. Canadell, R. L. Thompson, W. Winiwarter, P. Suntharalingam, *et al.*, A comprehensive quantification of global nitrous oxide sources and sinks, *Nature*, 2020, **586**, 248–256.
- IEA, *World Energy Outlook 2012*, International Energy Agency, Paris, 2012.
- IIASA 2012: *Global Energy Assessment – toward a Sustainable Future*, Cambridge University Press, Cambridge, 2012.
- IPCC, *Climate Change 2014: Mitigation of Climate Change, Contribution of Working Group III to the Fifth Assessment Report*, Cambridge University Press, Cambridge, UK & New York, NY, USA, 2014.
- T. Wei, J. Wu and S. Chen, Keeping Track of Greenhouse Gas Emission Reduction Progress and Targets in 167 Cities Worldwide, *Front. Sustain. Cities*, 2021, **3**, 696381.
- The Second Biennial Updated Report of Viet Nam to the United Nations Framework Convention on Climate Change*, Government of Vietnam, 2017.
- Nationally Determined Contribution (NDC), Government of Vietnam, 2022.
- Implementing Climate Ambition: Global Covenant of Mayors 2018 Global Aggregation Report*, published by the Global Covenant of Mayors for, Climate & Energy.
- Japan International Cooperation Agency, *Greenhouse Gas Inventory of Ho Chi Minh City, Project Report*, JICA, Japan, 2017.
- T. T. Q. Nguyen, W. Takeuchi, P. Misra and S. Hayashida, Technical note: Emission mapping of key sectors in Ho Chi Minh City, Vietnam, using satellite-derived urban land use data, *Atmos. Chem. Phys.*, 2021, **21**(4), 2795–2818.
- A. L. Eusebi, D. Cingolani, M. Spinelli, G. Passserini, S. Carletti and P. Battistoni, Dinitrogen oxide (N<sub>2</sub>O) emission in the treatment of urban wastewater via nitrite:



influence of liquid kinetic rates, *Water Sci. Technol.*, 2016, **74**, 2784–2794.

20 D. Tanikawa, K. Syutsubo, T. Watari, Y. Miyaoka, M. Hatamoto, S. Iijima, *et al.*, Greenhouse gas emissions from open-type anaerobic wastewater treatment system in natural rubber processing factory, *J. Clean. Prod.*, 2016, **119**, 32–37.

21 H. Arai, Y. Hosen, V. N. Pham Hong, N. T. Thi, C. N. Huu and K. Inubushi, Greenhouse gas emissions from rice straw burning and straw-mushroom cultivation in a triple rice cropping system in the Mekong Delta, *Soil Sci. Plant Nutr.*, 2015, **61**, 719–735.

22 A. T. Nguyen, J. Némery, N. Gratiot, T. S. Dao and T. T. M. Le, Does eutrophication enhance greenhouse gas emissions in urbanized tropical estuaries?, *Environ. Pollut.*, 2022, **303**, 119105.

23 M. Schmidt, H. Glatzel-Mattheier, H. Sartorius, D. E. Worthy and I. Levin, Western European N2O emissions: A top-down approach based on atmospheric observations, *J. Geophys. Res.*, 2001, **106**, 5507–5516.

24 A. Townsend-Small, D. E. Pataki, C. I. Czimczik and S. C. Tyler, Nitrous oxide emissions and isotopic composition in urban and agricultural systems in southern California, *J. Geophys. Res.*, 2011, **116**, G01013.

25 P. A. Barker, G. Allen, M. Flynn, S. Riddick and J. R. Pitt, Measurement of recreational N2O emissions from an urban environment in Manchester, UK, *Urban Clim.*, 2022, **46**, 101282.

26 K. Charoenpornpukdee, K. Stanely, J. Pitt, A. Wenger, A. Manning, D. Young, *et al.*, Recreational drug use as an urban source of nitrous oxide, *Environ. Sci.: Atmos.*, 2023, **3**, 962–969.

27 P. A. Dominutti, J. R. Hopkins, M. Shaw, G. P. Mills, L. Hoang Anh, H. H. Duong, *et al.*, Evaluating major anthropogenic VOC emission sources in densely populated Vietnamese cities, *Environ. Pollut.*, 2023, **318**, 120927.

28 H. To Thi, H. Duong Huu, P. A. Dominutti, D. Nguyen, C. Thien, J. R. Hopkins, *et al.*, Comprehensive volatile organic compound measurements and their implications for ground-level ozone formation in the two main urban areas of Vietnam, *Atmos. Environ.*, 2022, **269**, 118872.

29 H. To Thi, D. Nguyen, C. Thien, H. Duong Huu, L. Hoang Anh, D. E. Oram, *et al.*, Soluble trace metals associated with atmospheric fine particulate matter in the two most populous cities in Vietnam, *Atmos. Environ.: X*, 2022, **15**, 100178.

30 A. Garakani, R. J. Jaffe, D. Savla, A. K. Welch, C. A. Protin, E. O. Bryson, *et al.*, Neurologic, psychiatric, and other medical manifestations of nitrous oxide abuse: A systematic review of the case literature, *Am. J. Addict.*, 2016, **25**, 358–369.

31 S. Keddie, A. Adams, A. R. C. Kelso, B. Turner, K. Schmierer, S. Gnanapavan, *et al.*, No laughing matter: subacute degeneration of the spinal cord due to nitrous oxide inhalation, *J. Neurol.*, 2018, **265**, 1089–1095.

32 K. K. Patel, J. C. Mejia Munne, V. R. N. Gunness, D. Hersey, N. Alshafai, D. Sciubba, *et al.*, Subacute combined degeneration of the spinal cord following nitrous oxide anaesthesia: A systematic review of cases, *Clin. Neurol. Neurosurg.*, 2018, **173**, 163–168.

33 R. Chen, M. Liao and J. Ou, Laughing gas inhalation in Chinese youth: a public health issue, *Lancet Public Health*, 2018, **3**, 10.

34 D. Zheng, F. Ba, G. Bi, Y. Guo, Y. Gao and W. Li, The sharp rise of neurological disorders associated with recreational nitrous oxide use in China: a single-center experience and a brief review of Chinese literature, *J. Neurol.*, 2020, **267**, 422–429.

35 X. T. Dang, T. X. Nguyen, T. T. H. Nguyen and H. T. Ha, Nitrous Oxide-Induced Neuropathy among Recreational Users in Vietnam, *Int. J. Environ. Res. Publ. Health*, 2021, **18**, 6230.

36 Decree No. 137/2023/ND-CP, Viet Nam Government, 2023.

37 K. Q. Ngo, L. A. Hoang, B. Q. Ho, N. R. P. Harris, G. H. Drew and M. I. Mead, Street-scale dispersion modelling framework of road-traffic derived air pollution in Hanoi, Vietnam, *Environ. Res.*, 2023, **233**, 116497.

38 B. D. Hall, G. S. Dutton and J. W. Elkins, The NOAA nitrous oxide standard scale for atmospheric observations, *J. Geophys. Res.*, 2007, **112**, D9.

39 C. M. Silva, S. M. Corrêa and G. Arbillia, Determination of CO<sub>2</sub>, CH<sub>4</sub> and N<sub>2</sub>O: a Case Study for the City of Rio de Janeiro Using a New Sampling Method, *J. Braz. Chem. Soc.*, 2016, **27**(4), 778–786.

40 M. Biggart, J. Stocker, R. M. Doherty, O. Wild, M. Hollaway, D. Caruthers, *et al.*, Street-scale air quality modelling for Beijing during a winter 2016 measurement campaign, *Atmos. Chem. Phys.*, 2020, **20**, 2755–2780.

41 G. S. Dutton and B. D. Hall, *Global Atmospheric Nitrous Oxide Dry Air Mole Fractions from the NOAA GML Halocarbons in Situ Network, 1998–2023, Version: 2023-08-29*, 2023.

42 H. Hersbach, B. Bell, P. Berrisford, S. Hirahara, A. Horányi, J. Muñoz-Sabater, *et al.*, The ERA5 global reanalysis, *Q. J. R. Metereol. Soc.*, 2020, **146**(729), 1999–2049.

43 D. C. Carslaw, *The Openair Manual—Open-Source Tools for Analysing Air Pollution Data*, University of York, 2019.

44 L. L. Ashbaugh, W. C. Malm and W. Z. Sadeh, A residence time probability analysis of sulfur concentrations at Grand Canyon National Park, *Atmos. Environ.*, 1985, **19**(8), 1263–1270.

45 K. H. Becker, J. C. Lörzer, R. Kurtenbach, P. Wiesen, T. E. Jensen and T. J. Wallington, Nitrous Oxide (N<sub>2</sub>O) Emissions from Vehicles, *Environ. Sci. Technol.*, 1999, **33**(22), 4134–4139.

46 D. Famulari, E. Nemitz, C. Di Marco, G. J. Phillips, R. Thomas, E. House, *et al.*, Eddy-covariance measurements of nitrous oxide fluxes above a city, *Agric. For. Meteorol.*, 2010, **150**(6), 786–793.

47 Rampant Use of “Laughing Balls” in HCM City’s Bui Vien Pedestrian Street, *Vietnamnet Global*, 2022.

48 A. Banks and J. G. Hardman, Nitrous oxide, *Cont. Educ. Anaesth. Crit. Care Pain*, 2005, **5**, 145–148.

49 K. Knuf and C. V. Maani, *Nitrous Oxide. Treasure Island (FL)*, StatPearls Publishing, 2024.



50 C. J. Willmott, S. M. Robeson and K. Matsuura, A refined index of model performance, *Int. J. Climatol.*, 2011, **32**, 2088–2094.

51 *National Atmospheric Emissions Inventory, NAEI Website*, 2024.

52 M. Prigent and G. De Soete, Nitrous Oxide N<sub>2</sub>O in Engines Exhaust Gases - A First Appraisal of Catalyst Impact, *SAE Int.*, 1989, **94**(4), 281–291.

53 W. Zhang, H. Li, Q. Xiao and X. Li, Urban rivers are hotspots of riverine greenhouse gas (N<sub>2</sub>O, CH<sub>4</sub>, CO<sub>2</sub>) emissions in the mixed-landscape chaohu lake basin, *Water Res.*, 2021, **189**, 116624.

54 Z. Yu, H. Deng, D. Wang, M. Ye, Y. Tan, Y. Li, *et al.*, Nitrous oxide emissions in the Shanghai river network: implications for the effects of urban sewage and IPCC methodology, *Global Change Biol.*, 2013, **19**(10), 2999–3010.

55 E. Harris, S. Henne, C. Hüglin, C. Zellweger, B. Tuzson, E. Ibraim, *et al.*, Tracking nitrous oxide emission processes at a suburban site with semicontinuous, in situ measurements of isotopic composition, *J. Geophys. Res.: Atmos.*, 2017, **122**(3), 1850–1870.

56 C. Hood, J. Stocker, M. Seaton, K. Johnson, J. O'Neill, L. Thorne, *et al.*, Comprehensive evaluation of an advanced street canyon air pollution model, *J. Air Waste Manage. Assoc.*, 2021, **71**(2), 247–267.

57 W. Lv, Y. Wu and J. Zang, A Review on the Dispersion and Distribution Characteristics of Pollutants in Street Canyons and Improvement Measures, *Energies*, 2021, **14**(19), 6155.

58 S. Vardoulakis, B. E. Fisher, K. Pericleous and N. Gonzalez-Flesca, Modelling air quality in street canyons: A review, *Atmos. Environ.*, 2003, **37**(2), 155–182.

59 S. J. Kaar, J. Ferris, J. Waldron, M. Devaney, J. Ramsey and A. R. Winstock, Up: The rise of nitrous oxide abuse. An international survey of contemporary nitrous oxide use, *J. Psychopharmacol.*, 2016, **30**, 395–401.

60 O. Addington, Z. C. Zeng, T. Pongetti, R. L. Shia, K. R. Gurney, J. Liang, *et al.*, Estimating nitrous oxide (N<sub>2</sub>O) emissions for the Los Angeles Megacity using mountaintop remote sensing observations, *Rem. Sens. Environ.*, 2021, **259**, 112351.

61 M. G. M. Berges, R. M. Hofmann, D. Scharffe and P. J. Crutzen, Nitrous-Oxide Emissions from Motor-Vehicles in Tunnels and Their Global Extrapolation, *J. Geophys. Res. Atmos.*, 1993, **98**, 18527–18531.

62 M. E. Popa, M. K. Vollmer, A. Jordan, W. A. Brand, S. L. Pathirana, M. Rothe, *et al.*, Vehicle emissions of greenhouse gases and related tracers from a tunnel study: CO: CO<sub>2</sub>, N<sub>2</sub>O: CO<sub>2</sub>, CH<sub>4</sub>: CO<sub>2</sub>, O<sub>2</sub>: CO<sub>2</sub> ratios, and the stable isotopes <sup>13</sup>C and <sup>18</sup>O in CO<sub>2</sub> and CO, *Atmos. Chem. Phys.*, 2014, **14**, 2105–2123.

63 A. Sjodin, D. A. Cooper and K. Andreasson, Estimations of real-world N<sub>2</sub>O emissions from road vehicles by means of measurements in a traffic tunnel, *J. Air Waste Manag. Assoc.*, 1995, **45**, 186–190.

64 J. M. Dasch, Nitrous Oxide Emissions from Vehicles, *J. Air Waste Manage. Assoc.*, 1992, **42**, 63–67.

65 S. K. Hoekman, Review of Nitrous Oxide (N<sub>2</sub>O) Emissions from Motor Vehicles, *SAE Int. J. Fuels Lubr.*, 2020, **13**, 1.

66 J. Kim, A. A. Shusterman, K. J. Lieschke, C. Newman and R. C. Cohen, The Berkeley Atmospheric CO<sub>2</sub> Observation Network: field calibration and evaluation of low-cost air quality sensors, *Atmos. Meas. Tech.*, 2018, **11**, 1937–1946.

67 L. Spinelle, M. Gerboles, M. G. Villani, M. Aleixandre and F. Bonavitacola, Field calibration of a cluster of low-cost commercially available sensors for air quality monitoring. Part B: NO, CO and CO<sub>2</sub>, *Sens. Actuators, B*, 2017, **238**, 706–715.

68 M. I. Mead, O. A. M. Popoola, G. B. Stewart, P. Landshoff, M. Calleja, M. Hayes, *et al.*, The use of electrochemical sensors for monitoring urban air quality in low-cost, high-density networks, *Atmos. Environ.*, 2013, **70**, 186–203.

69 M. Mueller, J. Meyer and C. Hueglin, Design of an ozone and nitrogen dioxide sensor unit and its long-term operation within a sensor network in the city of Zurich, *Atmos. Meas. Tech.*, 2017, **10**, 3783–3799.

70 K. Bandara, K. Sakai, T. Nakandakari and K. Yuge, A Low-Cost NDIR-Based N<sub>2</sub>O Gas Detection Device for Agricultural Soils: Assembly, Calibration Model Validation, and Laboratory Testing, *Sensors*, 2021, **21**, 1189.

71 J. M. Fernandez, H. Maazallahi, J. L. France, M. Menoud, M. Corbu, M. Ardelean, *et al.*, Street-level methane emissions of Bucharest, Romania and the dominance of urban wastewater, *Atmos. Environ.*, 2022, **13**, 100153.

72 F. K. Kohler, C. Schaller and O. Klemm, Quantification of Urban Methane Emissions: A Combination of Stationary with Mobile Measurements, *Atmosphere*, 2022, **13**, 1596.

73 H. Maazallahi, A. Delre, C. Scheutz, A. M. Fredenslund, S. Schwietzke, H. Denier van der Gon, *et al.*, Intercomparison of detection and quantification methods for methane emissions from the natural gas distribution network in Hamburg, Germany, *Atmospheric Measurement Techniques Discussions* [preprint], 2022.

74 C. A. Woolley Maisch, J. L. France, R. E. Fisher, D. Lowry, G. Forster, T. Thi Hien, *et al.*, Identification of Sources of Methane in Ho Chi Minh City, Vietnam, *ACS Earth Space Chem.*, 2025, **9**(11), 2483–2492.

